

Piezoresistivity

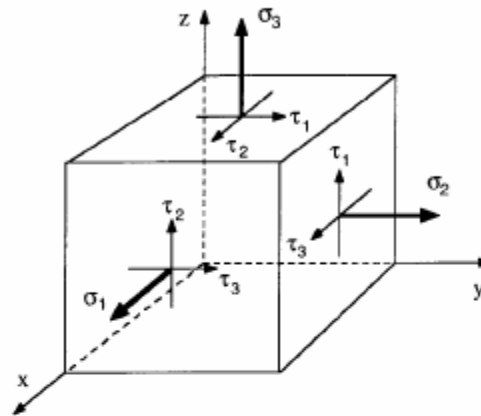
$$\begin{matrix} \text{Electric} & & & & & & \\ \text{Field} & \uparrow & & \uparrow & & \uparrow & \\ \begin{bmatrix} E_1 \\ E_2 \\ E_3 \end{bmatrix} & = & \begin{bmatrix} \rho_1 & \rho_6 & \rho_5 \\ \rho_6 & \rho_2 & \rho_4 \\ \rho_5 & \rho_4 & \rho_3 \end{bmatrix} & \cdot & \begin{bmatrix} i_1 \\ i_2 \\ i_3 \end{bmatrix} & \text{Current} \\ & & \text{Resistivity} & & & \\ & & \text{Tensor} & & & \end{matrix}$$

Resistivity is sensitive to stress: $\rho = \rho_{no \ stress} + \Delta\rho(\sigma, \tau)$

For cubic crystals (Si, Ge)

$$\frac{1}{\rho} \begin{bmatrix} \Delta\rho_1 \\ \Delta\rho_2 \\ \Delta\rho_3 \\ \Delta\rho_4 \\ \Delta\rho_5 \\ \Delta\rho_6 \end{bmatrix} = \begin{bmatrix} \pi_{11} & \pi_{12} & \pi_{12} & 0 & 0 & 0 \\ \pi_{12} & \pi_{11} & \pi_{12} & 0 & 0 & 0 \\ \pi_{12} & \pi_{12} & \pi_{11} & 0 & 0 & 0 \\ 0 & 0 & 0 & \pi_{44} & 0 & 0 \\ 0 & 0 & 0 & 0 & \pi_{44} & 0 \\ 0 & 0 & 0 & 0 & 0 & \pi_{44} \end{bmatrix} \cdot \begin{bmatrix} \sigma_1 \\ \sigma_2 \\ \sigma_3 \\ \tau_1 \\ \tau_2 \\ \tau_3 \end{bmatrix}$$

Piezoresistance in Silicon



$$E_1 = \rho \cdot i_1 + \rho\pi_{11}\sigma_1 \cdot i_1 + \rho\pi_{12}(\sigma_2 + \sigma_3) \cdot i_1 + \rho\pi_{44}(i_2\tau_3 + i_3\tau_2)$$

$$E_2 = \rho \cdot i_2 + \rho\pi_{11}\sigma_2 \cdot i_2 + \rho\pi_{12}(\sigma_1 + \sigma_3) \cdot i_2 + \rho\pi_{44}(i_1\tau_3 + i_3\tau_1)$$

$$E_3 = \rho \cdot i_3 + \rho\pi_{11}\sigma_3 \cdot i_3 + \rho\pi_{12}(\sigma_1 + \sigma_2) \cdot i_3 + \rho\pi_{44}(i_1\tau_2 + i_2\tau_1)$$

- These expressions are for bulk silicon
- For devices with finite dimensions, the influence of dimension changes need to be added through Poisson ratio

Quantum Mechanical Explanation

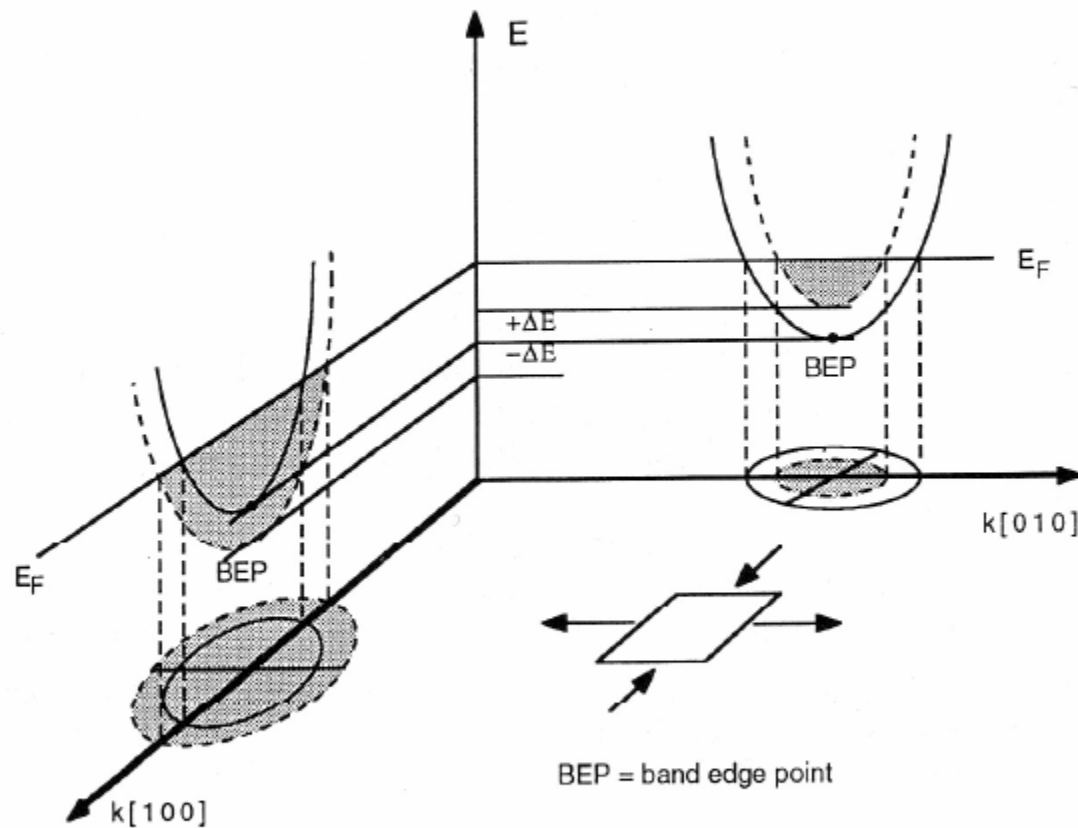
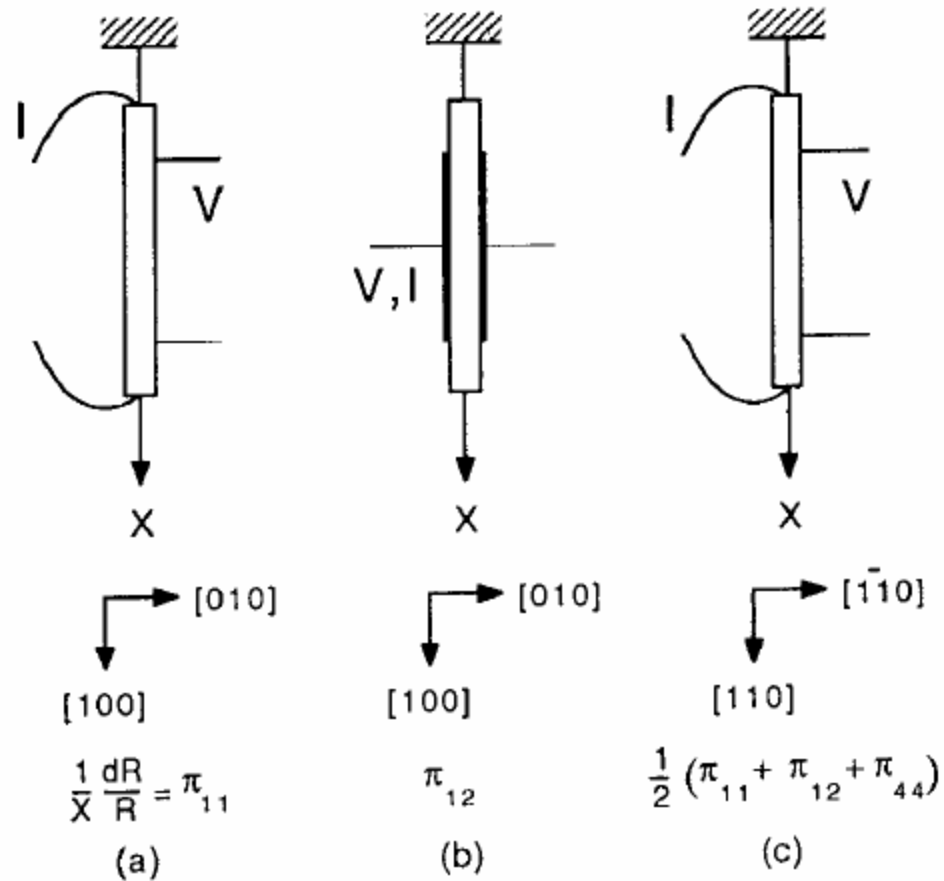
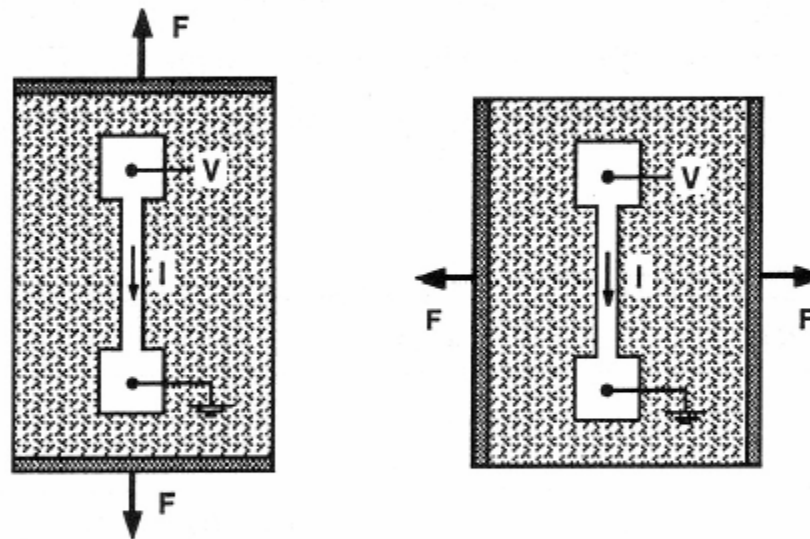


Fig. 7 Two n -type silicon valleys in k -space, aligned with the $[100]$ axes. E_F is the Fermi level. $+\Delta E$ is an energy increase and $-\Delta E$ an energy decrease.

Measurement of Piezoresistance Coefficients



Practical Piezoresistors



Longitudinal

Transverse

$$\frac{\Delta R}{R} = \pi_l \sigma_l + \pi_t \sigma_t$$

Longitudinal and Transverse Piezocoefficients in Directions Other Than Principal Axes

$$\begin{pmatrix} e_1 \\ e_2 \\ e_3 \end{pmatrix} = \begin{pmatrix} l_1 & l_2 & l_3 \\ m_1 & m_2 & m_3 \\ n_1 & n_2 & n_3 \end{pmatrix} \begin{pmatrix} u_1 \\ u_2 \\ u_3 \end{pmatrix}$$

Unit Vector for $\langle 100 \rangle$

Unit Vector for New Axes

$$\begin{pmatrix} x^* \\ y^* \\ z^* \end{pmatrix} = \begin{pmatrix} l_1 & l_2 & l_3 \\ m_1 & m_2 & m_3 \\ n_1 & n_2 & n_3 \end{pmatrix} \begin{pmatrix} x \\ y \\ z \end{pmatrix}$$

Vector in New Axes

$$E_1^* = l_1 E_1 + m_1 E_2 + n_1 E_3$$

$$E_1 = \rho \cdot i_1 + \rho \pi_{11} \sigma_1 \cdot i_1 + \rho \pi_{12} (\sigma_2 + \sigma_3) \cdot i_1 + \rho \pi_{44} (i_2 \tau_3 + i_3 \tau_2)$$

$$E_2 = \rho \cdot i_2 + \rho \pi_{11} \sigma_2 \cdot i_2 + \rho \pi_{12} (\sigma_1 + \sigma_3) \cdot i_2 + \rho \pi_{44} (i_1 \tau_3 + i_3 \tau_1)$$

$$E_3 = \rho \cdot i_3 + \rho \pi_{11} \sigma_3 \cdot i_3 + \rho \pi_{12} (\sigma_1 + \sigma_2) \cdot i_3 + \rho \pi_{44} (i_1 \tau_2 + i_2 \tau_1)$$

$$E^* = \rho \cdot i^* + \rho \cdot i^* \left[\pi_{11} + 2(\pi_{44} + \pi_{12} - \pi_{11})(l_1^2 m_1^2 + l_1^2 n_1^2 + m_1^2 n_1^2) \right]$$

$$\pi_l = \pi_{11} + 2(\pi_{44} + \pi_{12} - \pi_{11})(l_1^2 m_1^2 + l_1^2 n_1^2 + m_1^2 n_1^2)$$

Similarly

$$\pi_t = \pi_{12} - (\pi_{44} + \pi_{12} - \pi_{11})(l_1^2 l_2^2 + m_1^2 m_2^2 + n_1^2 n_2^2)$$

Longitudinal and Transverse Piezoresistance Coefficients in Cubic Crystals

ABLE 1 Longitudinal and Transverse Piezoresistance Coefficients for Various combinations of Directions in Cubic Crystals

| ongitudinal Direction | π_l | Transverse Direction | π_t |
|-----------------------|---|----------------------|--|
| (1 0 0) | π_{11} | (0 1 0) | π_{12} |
| (0 0 1) | π_{11} | (1 1 0) | π_{12} |
| (1 1 1) | $\frac{1}{3}(\pi_{11} + 2\pi_{12} + 2\pi_{44})$ | (1 $\bar{1}$ 0) | $\frac{1}{3}(\pi_{11} + 2\pi_{12} - \pi_{44})$ |
| (1 1 $\bar{0}$) | $\frac{1}{2}(\pi_{11} + \pi_{12} + \pi_{44})$ | (1 1 1) | $\frac{1}{3}(\pi_{11} + 2\pi_{12} - \pi_{44})$ |
| (1 1 $\bar{0}$) | $\frac{1}{2}(\pi_{11} + \pi_{12} + \pi_{44})$ | (0 0 1) | π_{12} |
| (1 1 0) | $\frac{1}{2}(\pi_{11} + \pi_{12} + \pi_{44})$ | (1 $\bar{1}$ 0) | $\frac{1}{2}(\pi_{11} + \pi_{12} - \pi_{44})$ |

Longitudinal and transverse piezoresistance coefficients are related to principle piezoresistance coefficients through coordinate transformation

Piezoresistance Coefficients for Si

| Type | Resistivity | π_{11} | π_{12} | π_{44} |
|--------|--------------------|----------------------------|----------------------------|----------------------------|
| Units | $\Omega\text{-cm}$ | 10^{-11} Pa^{-1} | 10^{-11} Pa^{-1} | 10^{-11} Pa^{-1} |
| n-type | 11.7 | -102.2 | 53.4 | -13.6 |
| p-type | 7.8 | 6.6 | -1.1 | 138.1 |

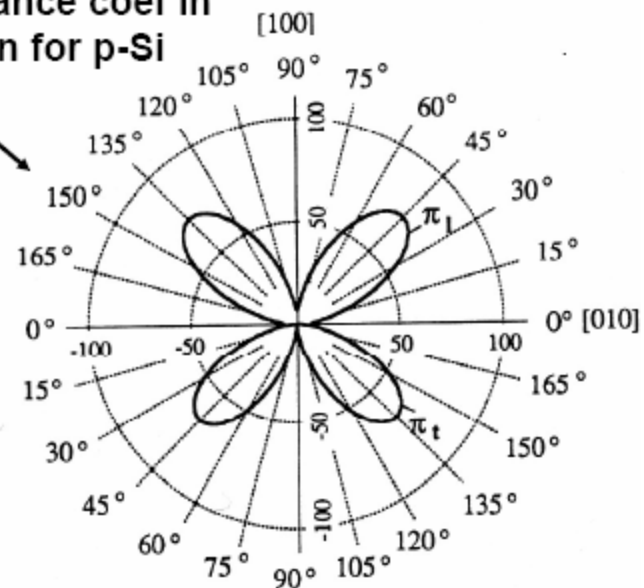
Longitudinal and transverse piezoresistance coef in a $\langle 100 \rangle$ plane as a function of orientation for p-Si

Maximum longitudinal
Piezoresistance coef:

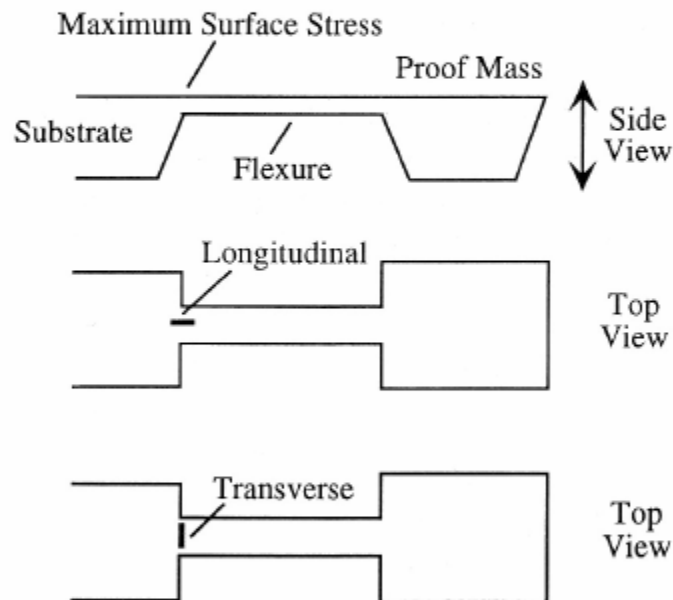
- p-Si: $\pi_{l\langle 111 \rangle} = 93.5 \times 10^{-11} \text{ Pa}^{-1}$

n-Si: $\pi_{l\langle 100 \rangle} = -102.2 \times 10^{-11} \text{ Pa}^{-1}$

→ p-Si is generally used because of orientation of anisotropic etching



Bulk-Micromachined Piezoresistive Accelerometers

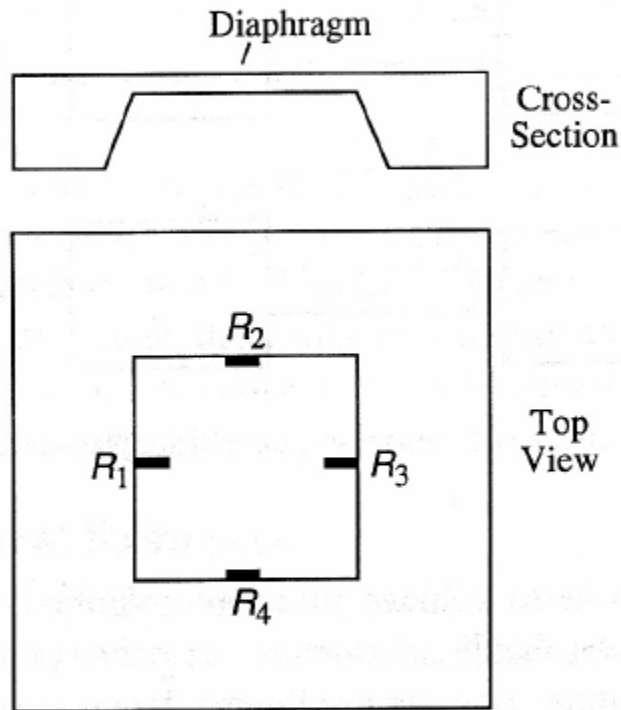


| | | |
|------|-----------------|-----------------|
| n-Si | $\pi_l = -31.2$ | $\pi_t = -17.6$ |
| p-Si | $\pi_l = 71.8$ | $\pi_t = -66.3$ |

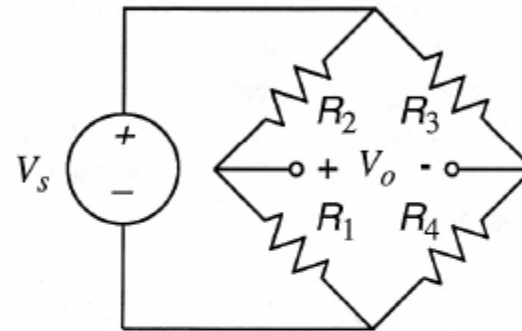
(Unit: 10^{-11} Pa^{-1})

Comparable magnitude, opposite sign
→ Suitable for bridge detection

Bulk-Micromachined Diaphragm Pressure Sensor



Wheatstone-bridge detection circuit:



$$R_1 = R_3 = (1 + \alpha_1)R_0$$

$$R_2 = R_4 = (1 - \alpha_2)R_0$$

$$\frac{V_o}{V_s} = \frac{R_1 R_3 - R_2 R_4}{(R_1 + R_2)(R_3 + R_4)} \approx \frac{2(\alpha_1 + \alpha_2)}{1 + \alpha_1 - \alpha_2}$$

$$\alpha_1 = (\pi_l + \nu \pi_t) \sigma_l = (67.7 \times 10^{-11}) \sigma_l$$

$$\alpha_2 = (\pi_t + \nu \pi_l) \sigma_l = (61.7 \times 10^{-11}) \sigma_l$$

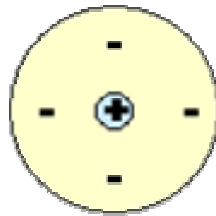
└─ Poisson ratio has a min. in [110], ~ 0.064

Piezoresistive

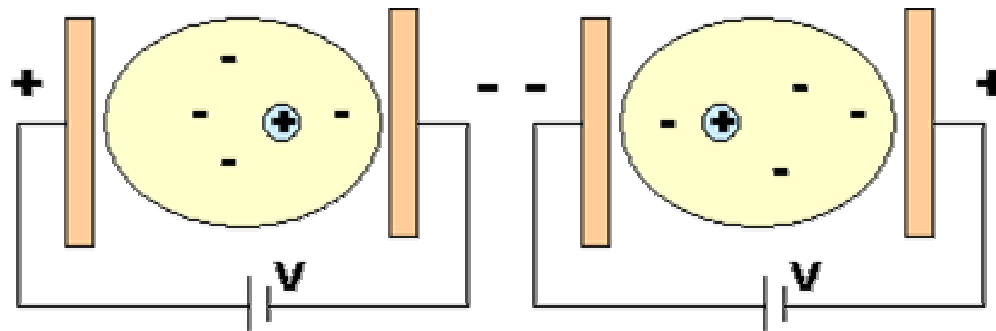
Materials: Silicon doped with impurities to make it n-type or p type

Applications: Accelerometer, strain gage

Electrostriction material

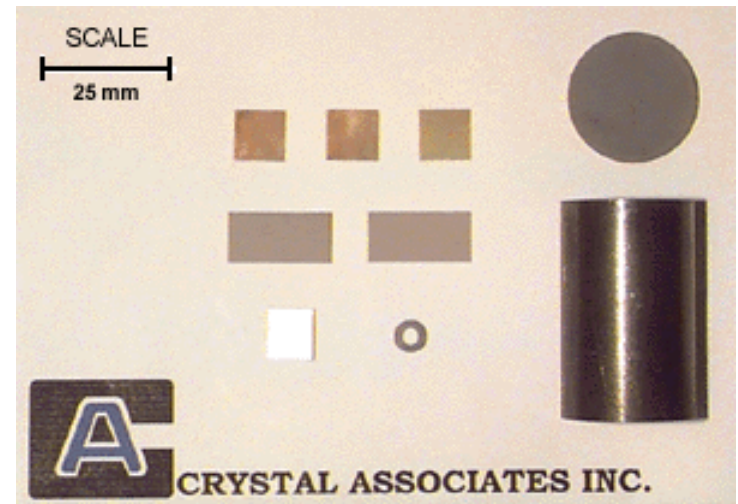
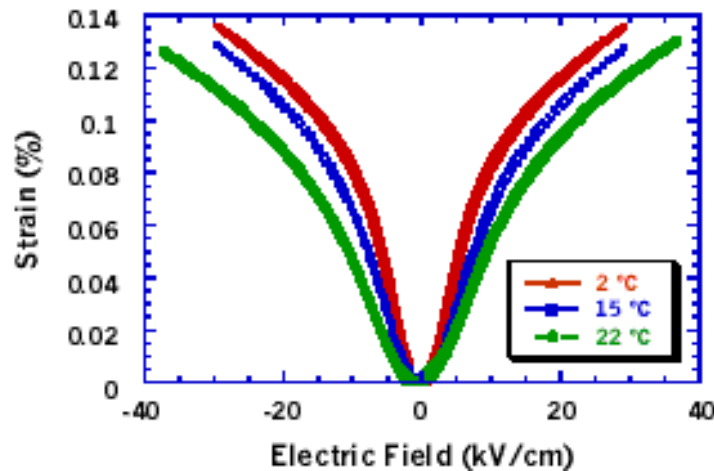


Neutral
atom



Electrostriction

- lead--magnesium--niobate (PMN) compositions
- ferroelectric



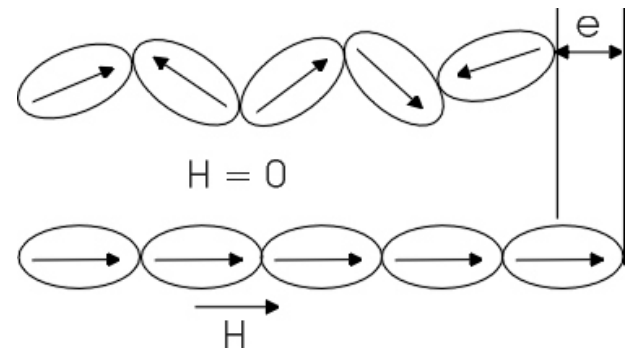
magnetostriction

Magnetostriction is the changing of a material's physical dimensions in response to changing its magnetization.

On a Macroscopic level may be segregated into two distinct processes:

The first process is dominated by the migration of domain walls within the material in response to external magnetic fields. Second, is the rotation of the domains.

These two mechanisms allow the material to change the domain orientation which in turn causes a dimensional change.



Magnetostrictive materials

Most ferromagnetic materials exhibit some measurable magnetostriction

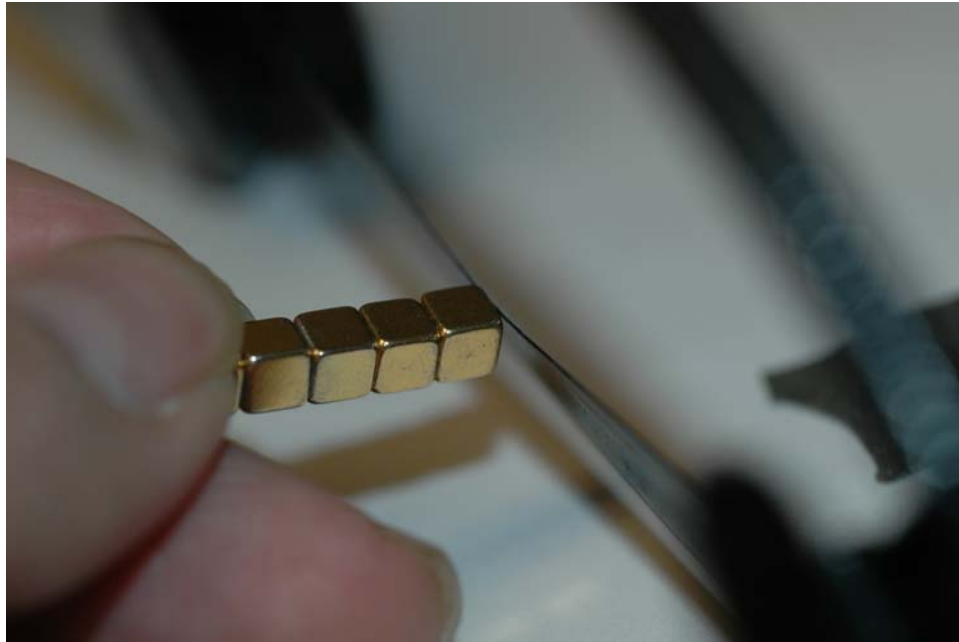
The ferromagnetic materials used in magnetostrictive sensors are transition metals such

- Cobalt
- Iron
- Nickel
- Ferrite

The highest room temperature magnetostriction of a pure element is that of Co which saturates at 60 microstrain.

highest known magnetostriction are those of cubic laves phase iron alloys containing the rare earth elements Dysprosium, Dy, or Terbium, Tb; DyFe₂, and TbFe₂. These alloys are generally stoichiometric, of the form Tb_xDy_{1-x}Fe₂ and have been coined Terfenol-D.

Ferromagnetic polymer



Resistive sensors and actuators

- Sensors
 - based on resistance change (either by physical mean or thermal induction)
- Actuators
 - based on thermal induction

thermal excitation

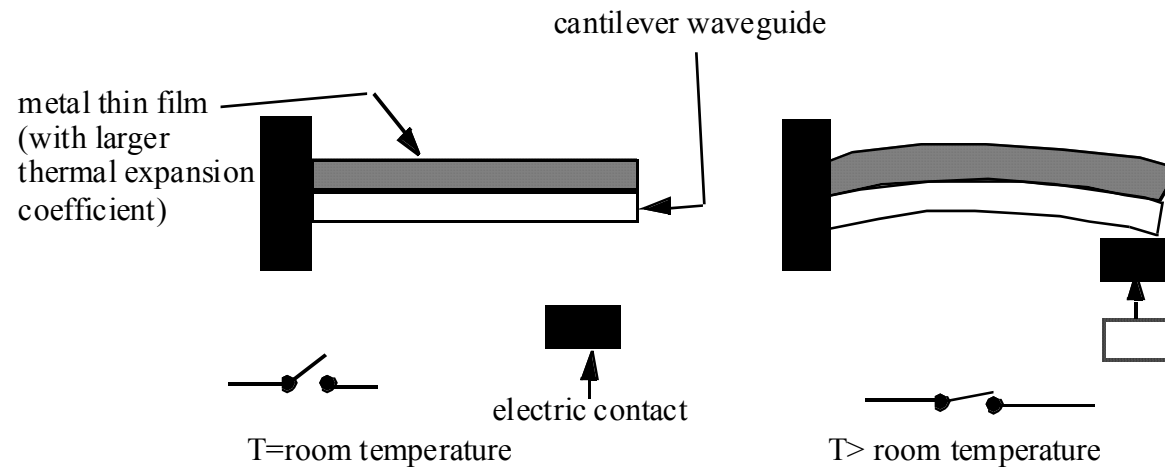
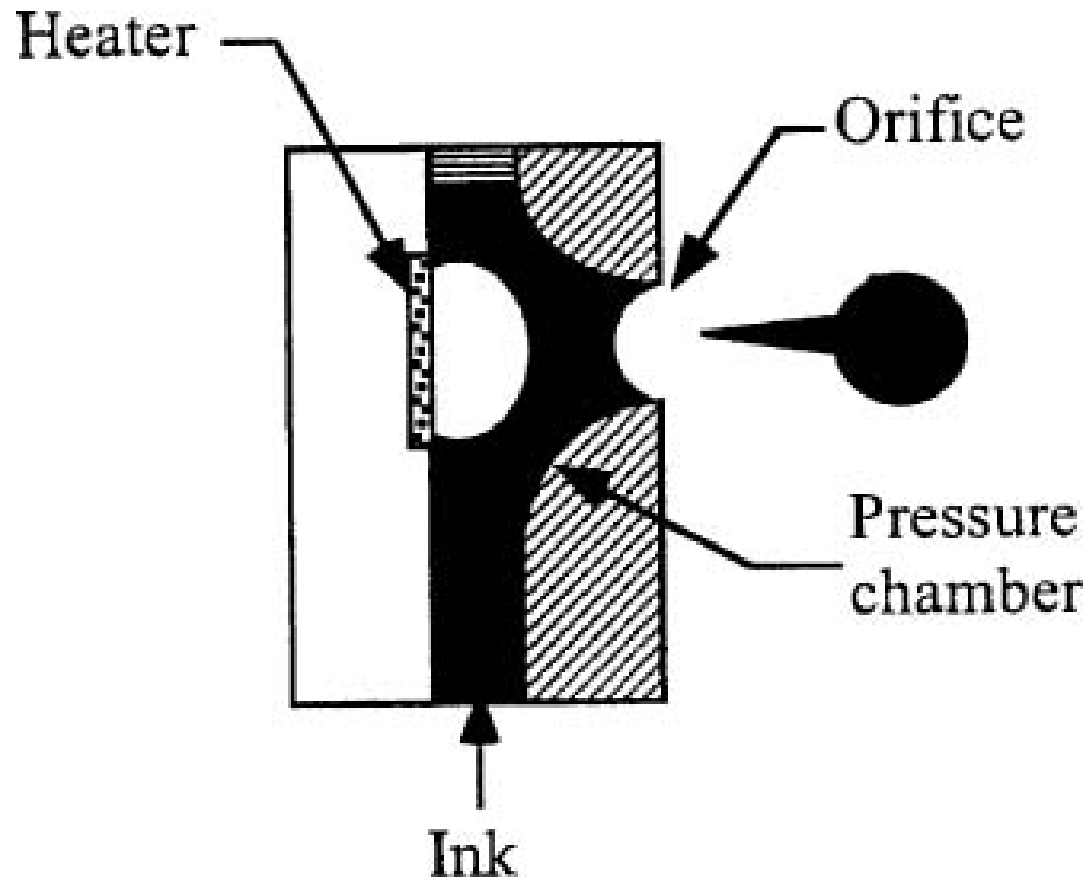
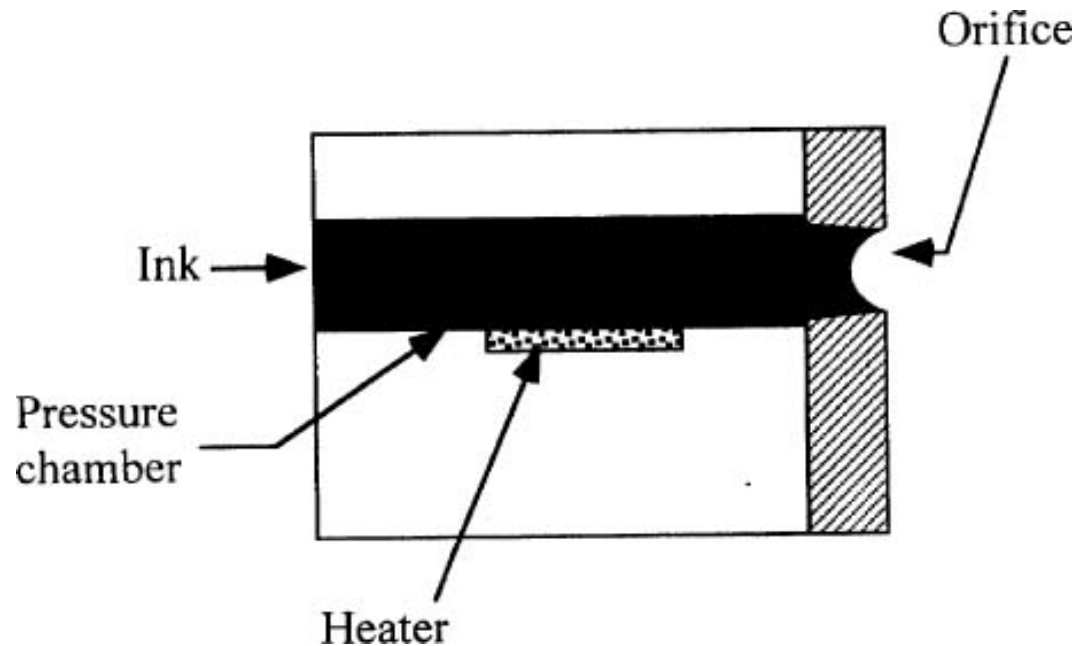


Figure 5a. Heat generated by electric conduction

Bubble jet printer head (roof shooter ink jet)



Side shooter thermal ink-jet



Opto-thermal excitation

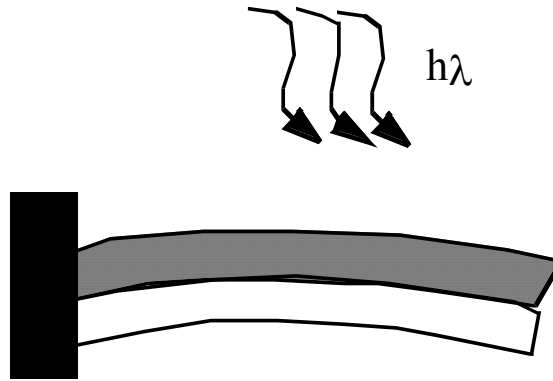
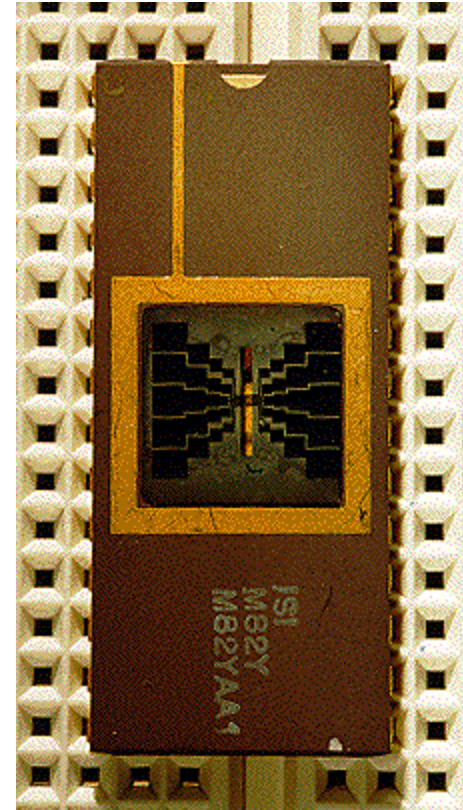
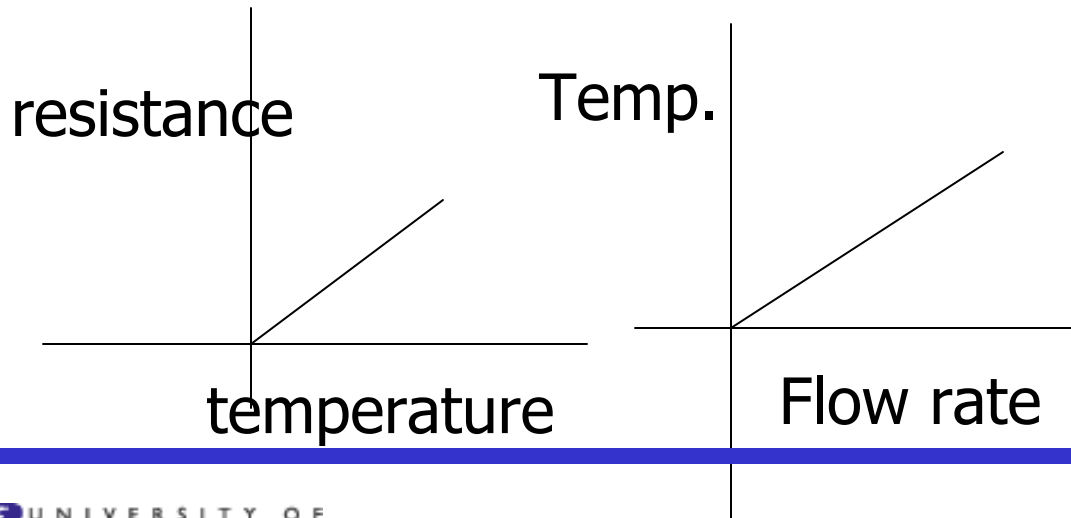
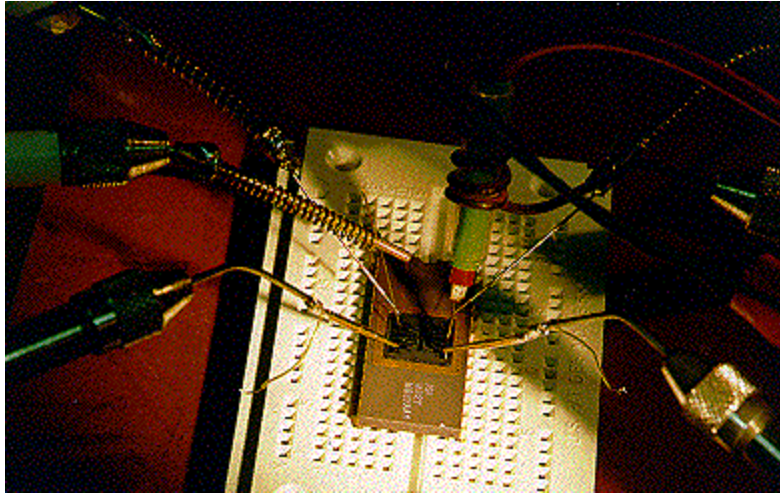


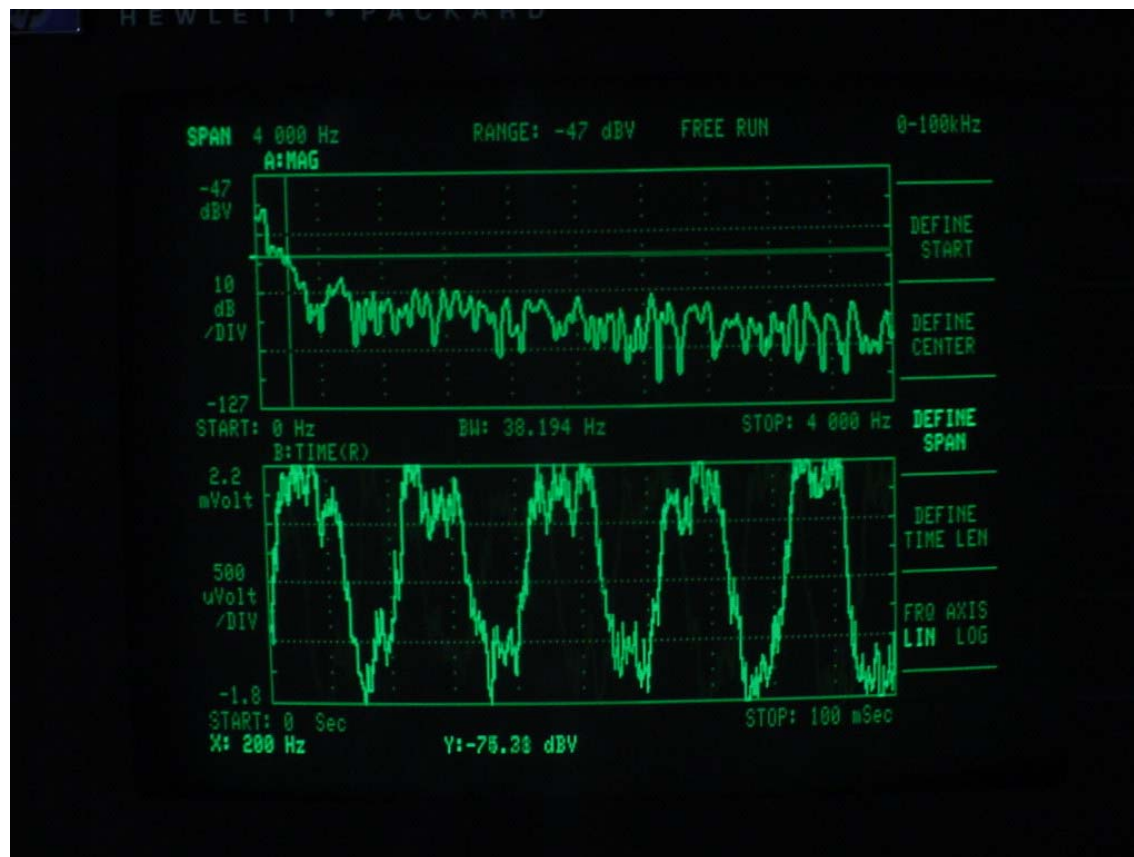
Figure 5b. Heat generated by light

use the effect of two different thermal expansions of sandwiched materials to obtain a desired movement when the temperature of the assembly is changed

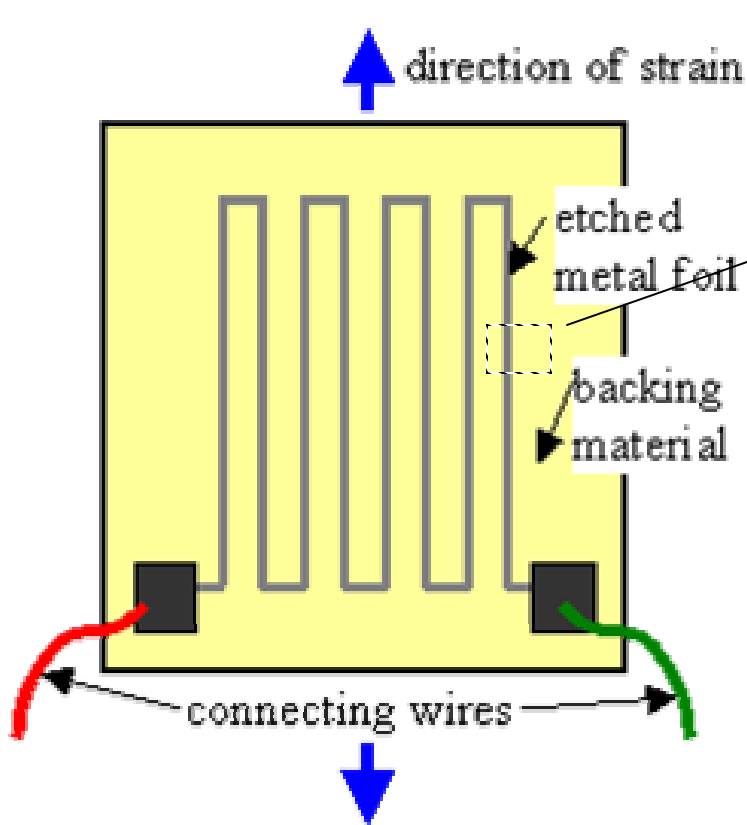
MEMS acoustic sensor-hotwire sensor (thermo-resistor)



Experimental results



Strain gages (resistive sensors)

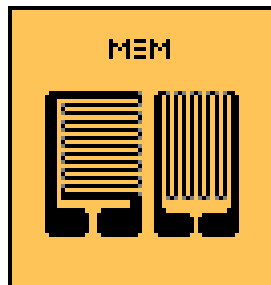


- The electrical resistance of a wire changes with strain:
- As strain increases, the wire length L increases, which increases R .
- As strain increases, the wire cross-sectional area A decreases, which increases R .
- For most materials, as strain increases, the wire resistivity also increases, which further increases R .

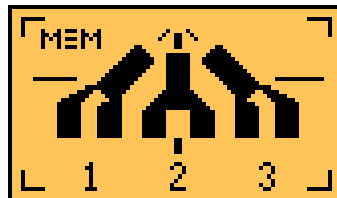
Strain gage types

- Metallic
- Copper-nickel (static strain meas.)
- Nickel-chrome (static and dynamic higher temp alloy)
- Nickel-ion high gage facto (dynamic)
- Platinum alloy (superior stability and fatigue resistance at high temperatures)
- Semiconductor
- P type (Boron doped) or n type (Phosphorus)
- Change density change with strain
- Resistance can either decrease or increase with applied strain
- Low hysteresis
- Smaller in size
- High gage factor (sensitivity)

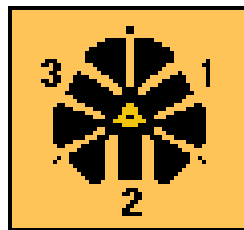
Wire and foil strain gage



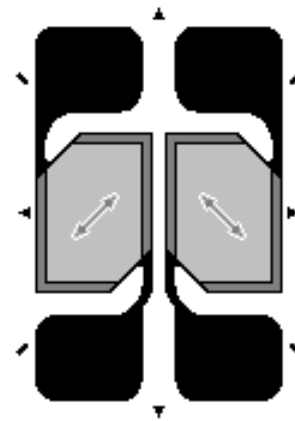
0° - 90°
"Tee"
Rosette



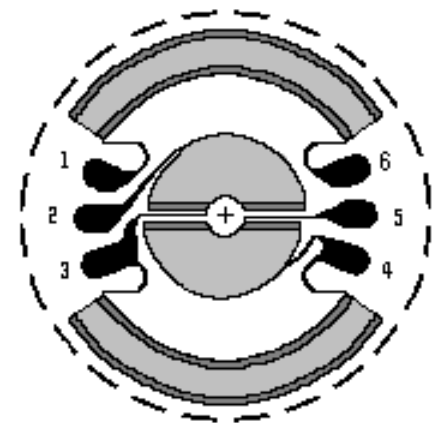
0° - 45° - 90°
Rectangular
Rosette



0° - 60° - 120°
Delta
Rosette

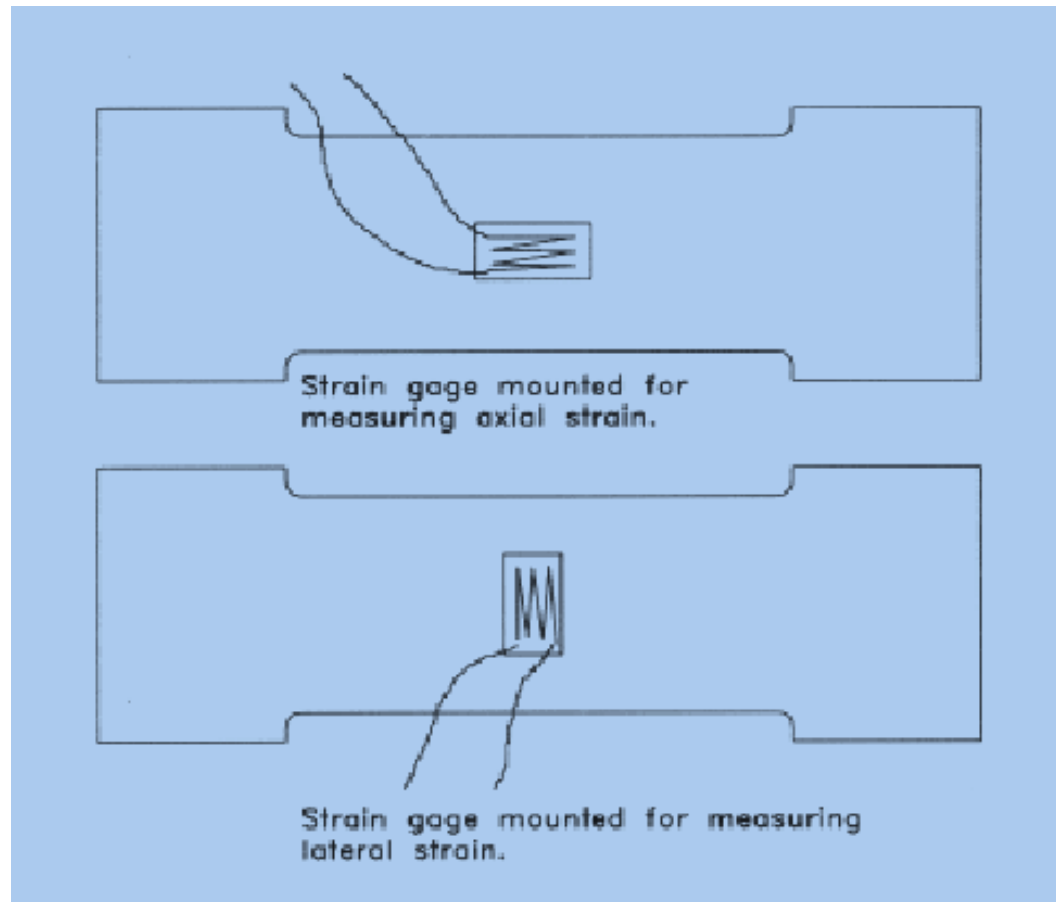


Shear gage



Full bridge diaphragm gage

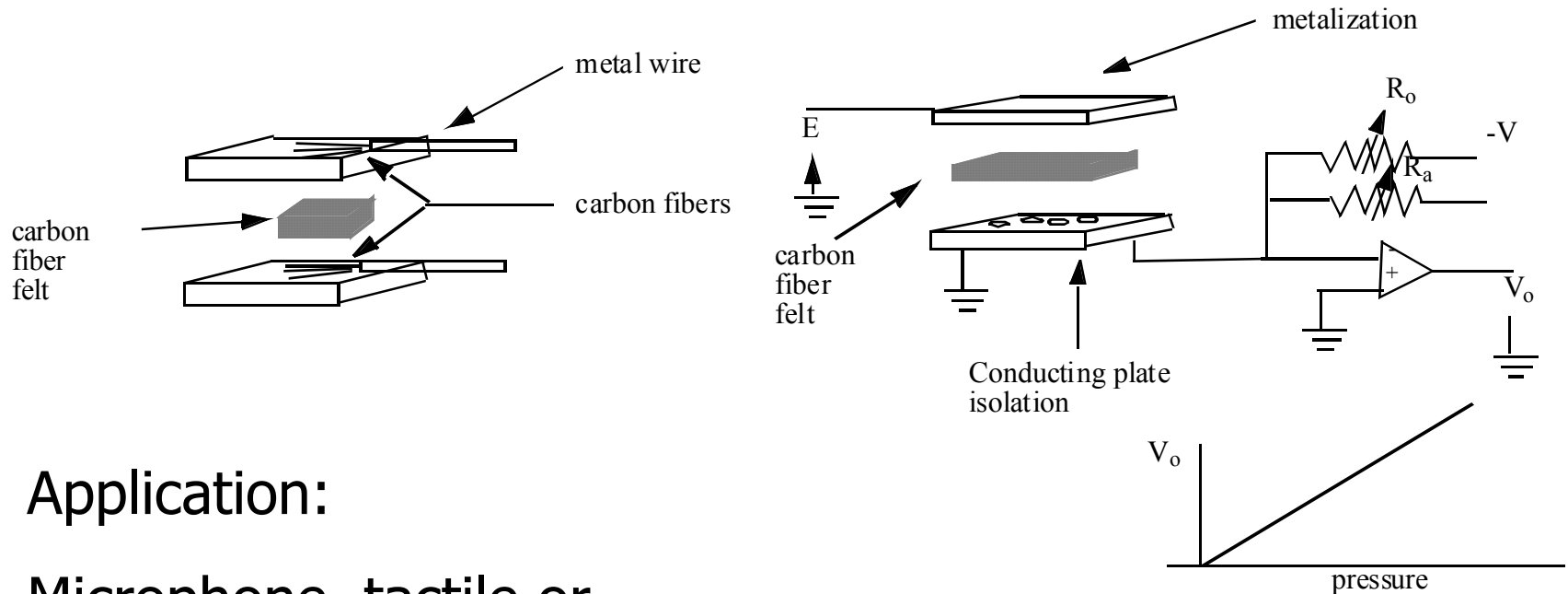
Application of strain gage



Gage factor

- Gage factor $GF = (\Delta R/R)/(\Delta L/L)$

Carbon fibers filled sensor (resistive sensor)



Application:

Microphone, tactile or pressure sensor...

Carbon fibers filled resistive sensor

Advantages:

- excellent strength, stiffness, elasticity, fatigue
- flexibility: can be fitted to any shape

Low hysteresis (5%)

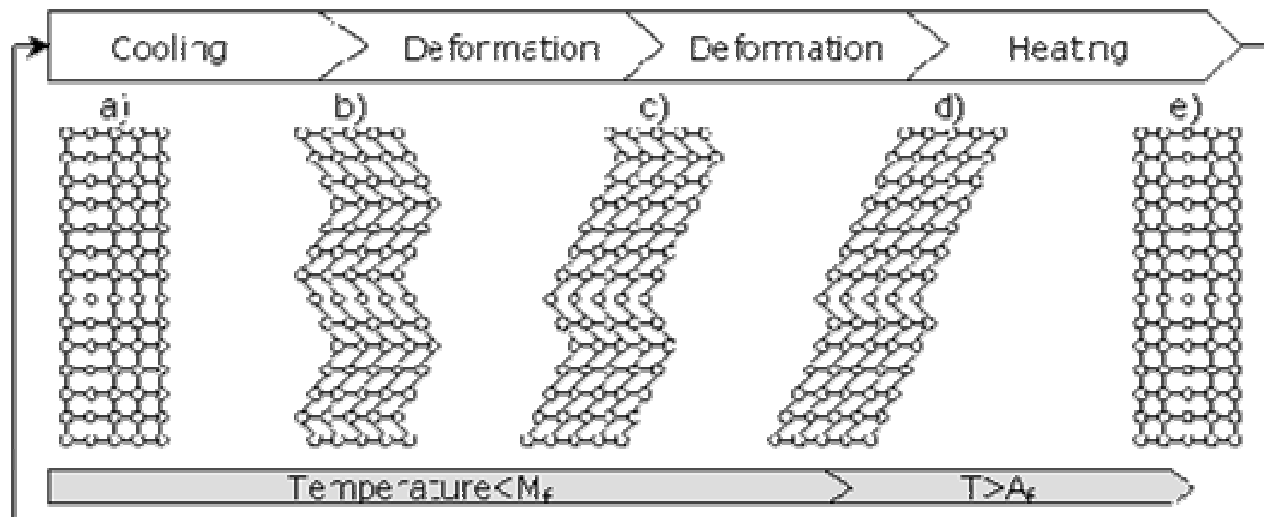
- thermal stability: high thermal stability $>500^{\circ}\text{C}$
- inexpensive

Disadvantages:

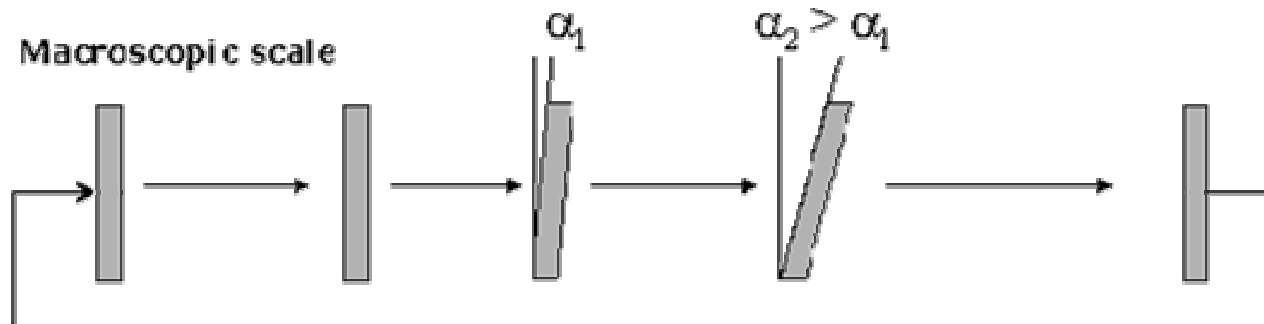
- Thermal conductivity and thermal expansion are low
- Noise: fibers in contact with metals generate noise

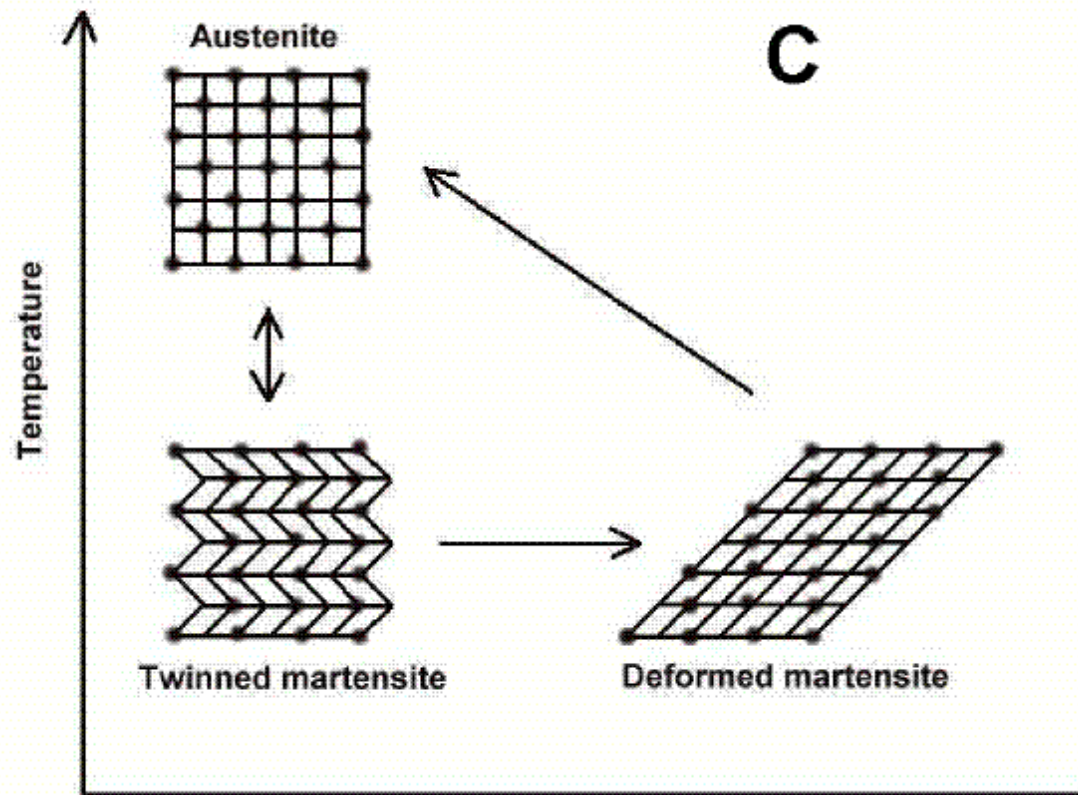
Shape memory actuator

Microscopic scale



Macroscopic scale





SMA

Materials:

- mostly Ni/Ti alloy, but also Au/Cu. In/Ti

Advantages:

- considerable temperature dependent expansion/contraction
- relatively linear control
- Very high stress ($>200\text{MPa}$)
- Arbitrary shape
- Simple actuation
- Life time-millions of cycles

SMA

Disadvantages:

- special alloy
- high annealing temperature ($\sim 400^{\circ}\text{C}$)
- long time constant (time delay)

Shape memory alloy application

- Cloth insert (Brassiere Underwires)
- Medical implant (vascular stents)
- Temperature sensors or switches
- Damping device
- Micro-actuator
- Smart structure



Twist and slide actuator



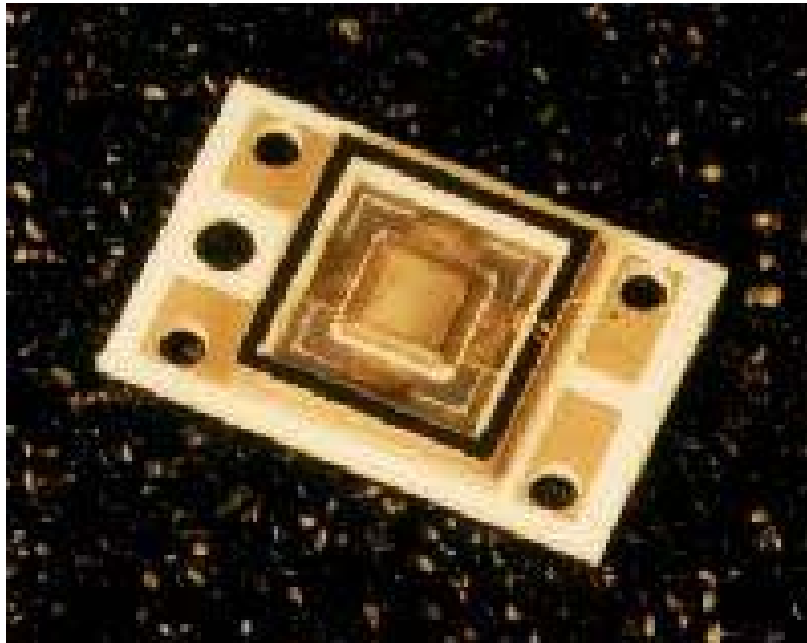
Ferromagnetic Shape memory alloys FSMA

FSMAs are ferromagnetic alloys which also support the shape memory effect, undergo the characteristic martensitic transformation upon cooling, and show all features of conventional shape

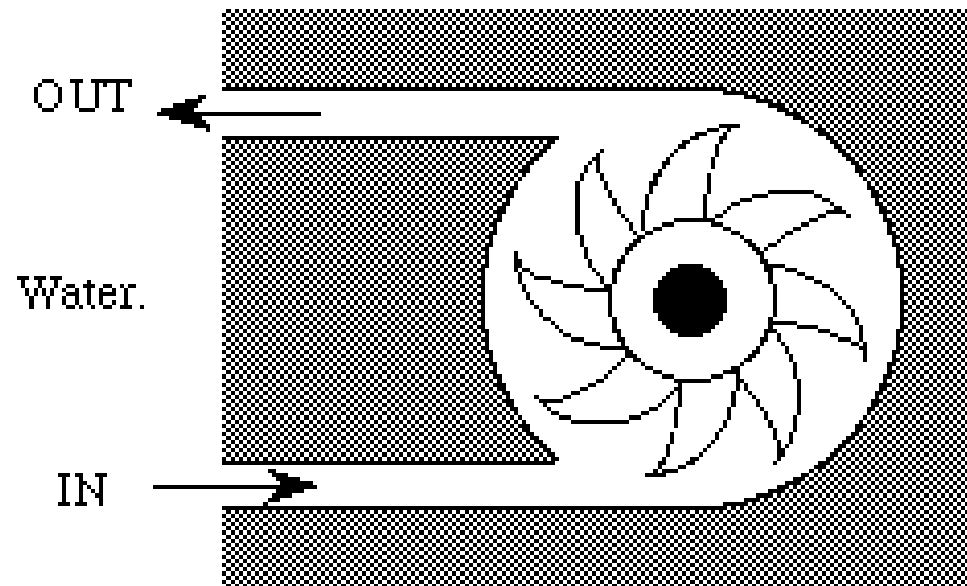
- actuation mechanism are magnetically driven (3KG and larger). This difference allows for increased frequency response (fast actuation).
- large strains (around 6%).

only alloys in the Ni-Mn-Ga

Micro-Pneumatic Valve



Hydraulic actuator



Potential s a lot of power can be delivered from an external souce along very narrow diameter tubes.